Journal of Solid State Chemistry 183 (2010) 849–857

Contents lists available at ScienceDirect

Journal of Solid State Chemistry

journal homepage: www.elsevier.com/locate/jssc

Auxiliary aromatic-acid effect on the structures of a series of Zn^{II} coordination polymers: Syntheses, crystal structures, and photoluminescence properties

Yan-Hong Xu, Ya-Qian Lan *, Kui-Zhan Shao, Zhong-Min Su *, Yi Liao *

Institute of Functional Material Chemistry, Faculty of Chemistry, Northeast Normal University, Changchun 130024, PR China

ARTICLE INFO

Article history:
Received 31 July 2009
Received in revised form
3 January 2010
Accepted 24 January 2010
Available online 1 February 2010

Keywords:
(Pyridyl)imidazole derivative ligand
Aromatic-acid ligands
Zn^{II}
Topology
Luminescent property

ABSTRACT

Five novel Zn^{II}-(pyridyl)imidazole derivative coordination polymers, $[Zn(L)_2]$ (**1**), $[Zn_2(\mu_3\text{-OH})L(m\text{-BDC})]$ (**2**), $[Zn_2(\mu_3\text{-OH})L(p\text{-BDC})]\cdot H_2O$ (**3**), $[Zn_2L(BTC)(H_2O)]\cdot 2.5H_2O$ (**4**) and $[Zn_{3.5}(\mu_3\text{-OH})L_2(BTEC)(H_2O)]\cdot H_2O$ (**5**) (L=4-((2-(pyridine-2-yl)-1*H*-imidazol-1-yl)methyl)benzoic acid, p-H_2BDC=1,4-benzenedicarboxylic acid, m-H_2BDC=1,3-benzenedicarboxylic acid, H_3BTC=1,3,5-benzenetricarboxylic acid, H_4BTEC=1,2,4,5-benzenetetracarboxylic acid), were successfully synthesized under hydrothermal conditions through varying auxiliary aromatic-acid ligands and structurally characterized by X-ray crystallography. Compound **1** exhibits a 1D chain linked via double L bridges. Compound **2** features a well-known pcu topology with bent dicarboxylate ligand (m-H_2BDC) as an auxiliary ligand, while **3** displays a bcu network with linear dicarboxylate ligand (p-H_2BDC) as an auxiliary ligand. The structure of compound **4** is a novel 3D (3,5)-connected network with $(4\cdot6^2)(4\cdot6^4\cdot8^2\cdot10\cdot12^2)$ topology. It is interesting that compound **5** shows an intricate (3,4,8)-connected framework with $(4\cdot6^2)(4^2\cdot6^3\cdot8)(4^2\cdot6^4)(4^2\cdot6^{18}\cdot7\cdot8^6\cdot10)$ topology. In addition, their infrared spectra (IR), X-ray powder diffraction (XPRD) and photoluminescent properties were also investigated in detail.

1. Introduction

The rational design and synthesis of metal-organic frameworks (MOFs) is of current interest in the field of crystal engineering and supramolecular chemistry. This is justified not only by their intriguing variety of architectures and topologies, such as rectangular grids, herringbones, boxes, ladders, brick walls, rings, diamondoids, and honeycombs, but also by their potential applications in ion-exchange, non-linear optics, molecular sieves, gas storage, catalysis, magnetism, and molecular sensing [1–6]. Although a variety of MOFs with beautiful topologies and interesting properties have been synthesized to date, rational control in the construction of polymeric networks still remains a great challenge in crystal engineering. From the viewpoint of crystal engineering, the most effective and facile approach to overcome this is the appropriate choice of the well-designed organic bridging ligands (building blocks) containing modifiable backbones and connectivity information, together with the metal centers (nodes) with various coordination preferences [7–9]. Multidentate N- or O-donor ligands have been investigated extensively as organic spacers in the construction of MOFs. Such as, the use of 4,4′-bipyridine [10,11], imidazole [12,13] and their analogs [14–17], as neutral N-donor ligands, are excellent organic ligands towards the syntheses of extended multidimensional coordination polymers due to their simple bridging fashion and strong coordination ability to transition metal ions. In the meantime, di- [18,19] or polycarboxylate [20,21] ligands, as O-donor ligands via anionic groups, are another kind of candidates for the preparation of multidimensional coordination networks, owing to the rich coordination modes of the carboxylate groups, and can afford neutral MOFs. According to the above considerations, we incorporated both neutral and anionic donor groups into a single organic ligand, namely, 4-((2-(pyridine-2-yl)-1*H*-imidazol-1-yl)-methyl)benzoic acid (L), as shown in Scheme 1. From a structural point of view, it should be pointed out that (i) this ligand, which possesses flexibility owing to the presence of a $-CH_2-$ spacer between (pyridyl)imidazole ring and carboxylate terminal, can freely rotate to meet the requirement of coordination geometries of metal ions in the assembly process; (ii) the L ligand contains remarkable coordination abilities (both N- and O-donor sites), it is able to react with transition metal ions to produce unique structural motifs with beautiful aesthetics and useful functional properties; (iii) it has an asymmetric geometry that may lead to unprecedented structures with novel topological features.

Meanwhile, it is well-known that many factors influence the formation of the final architectures in molecular self-assembly

* Corresponding authors. Fax: +86 431 5684009.
E-mail address: zmsu@nenu.edu.cn (Z.-M. Su).

0022-4596/$ - see front matter © 2010 Elsevier Inc. All rights reserved.
doi:10.1016/j.jssc.2010.01.027

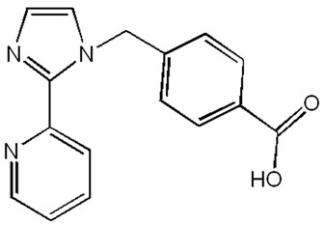

Scheme 1. Conformation of flexible ligand L.

processes, such as the solvent system, template, central metal, and anion [22–24]. We are particularly interested in the effects of auxiliary anions on the architectures of the final compounds. So far, although the effect of anions on the structures of compounds has been studied, systematic investigations on the influence of organic anions such as aromatic polycarboxylate ligands on their compound structures have been lacking [25–27].

In this work, through precise control of organic-acid linker structural features such as dentation and shape, in the absence or presence of auxiliary aromatic polycarboxylate ligands, a remarkable class of Zn^{II} compounds with rich architectures has been obtained: $[Zn(L)_2]$ (**1**), $[Zn_2(\mu_3\text{-}OH)L(m\text{-}BDC)]$ (**2**), $[Zn_2(\mu_3\text{-}OH)L(p\text{-}BDC)]\cdot H_2O$ (**3**), $[Zn_2L(BTC)(H_2O)]\cdot 2.5H_2O$ (**4**) and $[Zn_{3.5}(\mu_3\text{-}OH)L_2(BTEC)(H_2O)]\cdot H_2O$ (**5**). On the basis of synthesis and structural characterization, the influence of auxiliary aromatic ligands on controlling of the final compound structures is discussed. Furthermore, the role of weak intermolecular force such as aromatic π–π stacking interaction in the creation of molecular architectures has also been investigated for the compound **1**.

2. Experimental section

2.1. Materials and general methods

All commercially available chemicals are of reagent grade and used as received without further purification. (2-(2-pyridyl)imidazole) was synthesized according to the reported procedure [28,29]. FT-IR spectra were recorded from KBr pellets in the range of 400–4000 cm^{-1} on a Mattson Alpha-Centauri spectrometer. Elemental analyses of carbon, hydrogen and nitrogen were carried out with a Carlo Erba 1106 elemental analyzer. Thermal gravimetric analyses (TGA) were performed on a Perkin-Elmer TG-7 instrument in flowing N_2 with a heating rate of 10 °C/min. The emission/excitation spectra were recorded on a Varian Cary Eclipse spectrometer. X-ray powder diffraction (XRPD) patterns were recorded on a Siemens D5005 diffractometer with Cu KR (λ=1.5418 Å) radiation.

2.2. Synthesis of 4-((2-(pyridine-2-yl)-1H-imidazol-1-yl)methyl)benzoic acid (L)

Solution containing 2-(2-pyridyl)imidazole (0.01 mol) and NaOH (0.02 mol) in DMF (25 mL) was heated at 60 °C for 30 min. Then, 4-(chloromethyl)benzonitrile (0.01 mol) was added directly, and the mixture was continuously stirred and heated for 10 h. After cooling, the mixture was precipitated with 200 mL of distilled water and then the light-brown solid of (4-((2-(pyridine-2-yl)-1*H*-imidazol-1-yl)methyl)benzonitrile) was obtained. A mixture of 4-((2-(pyridine-2-yl)-1*H*-imidazol-1-yl)methyl)benzonitrile (50 mmol) and NaOH (200 mmol) in H_2O (200 mL) was stirred at 100 °C for 12 h, and was cooled to room temperature. Then the mixture was adjusted to pH ≈ 5 with HCl (1.0 mol L^{-1}), and a white solid of L formed immediately, which was isolated by filtration in 80% yield after drying in air. Anal. Calcd. for $C_{16}H_{13}N_3O_2$: C, 66.84; H, 4.66; N, 15.04. Found: C, 66.76; H, 4.59; N, 15.11%. IR data (KBr, cm^{-1}): 3432s, 3115s, 1706s, 1587s, 1488s, 1463s, 1411s, 1307m, 1153w, 1090w, 939s, 793s, 770s, 703s, 461m. ^1H NMR (DMSO): 8.51 (d, 1H, *J*=1.06 Hz), 8.05 (t, 1H, *J*=1.00 Hz), 7.86 (d, 1H, *J*=0.96 Hz), 7.83 (d, 1H, *J*=2.28 Hz), 7.43 (d, 1H, *J*=0.98Hz), 7.31 (d, 1H, *J*=1.04 Hz), 7.20 (d, 1H, *J*=2.19 Hz), 7.11 (d, 1H, *J*=1.04 Hz), 5.95 (s, 2H, *J*=2.24 Hz, $-CH_2-$). The carboxylate-bound hydrogen was not detected.

2.3. Synthesis of compounds 1–5

$[Zn(L)_2]$ (1). To 10 mL of distilled water was added $Zn(OAc)_2\cdot 2H_2O$ (0.2 mmol) and L (0.1 mmol) while stirring. When the pH value of the mixture was adjusted to about 7.0 with NaOH solution (1.0 mol L^{-1}), then the mixture was placed in a 23 mL Teflon-lined stainless steel vessel, and heated at 150 °C for 72 h, and then the reaction system was cooled to room temperature at a rate of 5 °C/h. Crystals of **1** were obtained in yield (based on Zn): 54%. Anal. Calcd. for $C_{32}H_{24}N_6O_4Zn$: C, 61.79; H, 3.88; N, 13.51%. Found: C, 61.82; H, 3.85; N, 13.54%. IR data (KBr, cm^{-1}): 3003s, 1621s, 1569s, 1473s, 1416s, 1363s, 1288s, 990s, 858s, 790s, 701s, 622s 548s, 498s.

$[Zn_2(\mu_3\text{-}OH)L(m\text{-}BDC)]$ (**2**). To 10 mL of distilled water was added $Zn(OAc)_2\cdot 2H_2O$ (0.2 mmol), *m*-H_2BDC (0.1 mmol) and L (0.1 mmol) while stirring. When the pH value of the mixture was adjusted to about 6.5 with NaOH solution (1.0 mol L^{-1}), then the mixture was placed in a 23 mL Teflon-lined stainless steel vessel, and heated at 150 °C for 72 h, and then the reaction system was cooled to room temperature at a rate of 5 °C/h. Crystals of **2** were obtained in yield (based on Zn): 72%. Anal. Calcd. for $C_{24}H_{17}N_3O_7Zn_2$: C, 48.92; H, 2.73; N, 7.13%; Found: C, 48.97; H, 2.69; N, 7.09%. IR data (KBr, cm^{-1}): 3113s, 1614s, 1563s, 1477s, 1397s, 1362s, 1187s, 1153s, 960s, 784s, 742s, 715s, 444s.

$[Zn_2(\mu_3\text{-}OH)L(p\text{-}BDC)]\cdot H_2O$ (**3**). To 10 mL of distilled water was added $Zn(OAc)_2\cdot 2H_2O$ (0.2 mmol), *p*-H_2BDC (0.1 mmol) and L (0.1 mmol) while stirring. When the pH value of the mixture was adjusted to about 6.5 with NaOH solution (1.0 mol L^{-1}), then the mixture was placed in a 23 mL Teflon-lined stainless steel vessel, and heated at 150 °C for 72 h, and then the reaction system was cooled to room temperature at a rate of 5 °C/h. Crystals of **3** were obtained in yield (based on Zn): 77%. Anal. Calcd. for $C_{24}H_{19}N_3O_8Zn_2$: C, 47.47; H, 2.98; N, 6.92%. Found: C, 47.51; H, 2.92; N, 6.97%. IR data (KBr, cm^{-1}): 3742s. 3591s, 3115s, 1604s, 1568s, 1500s, 1478s, 1404s, 1288s, 1152s, 1011s, 890s, 848s, 786s, 740s, 585s, 447s.

$[Zn_2L(BTC)(H_2O)]\cdot 2.5H_2O$ (**4**). To 10 mL of distilled water was added $Zn(OAc)_2\cdot 2H_2O$ (0.2 mmol), H_3BTC (0.1 mmol) and L (0.1 mmol) while stirring. When the pH value of the mixture was adjusted to about 6.0 with NaOH solution (1.0 mol L^{-1}), then the mixture was placed in a 23 mL Teflon-lined stainless steel vessel, and heated at 150 °C for 72 h, and then the reaction system was cooled to room temperature at a rate of 5 °C/h. Crystals of **4** were obtained in yield (based on Zn): 63%. Anal. Calcd. for $C_{200}H_{176}N_{24}O_{92}Zn_{16}$: C, 44.17; H, 3.23; N, 6.18%. Found: C, 44.26; H, 3.17; N, 6.14%. IR data (KBr, cm^{-1}): 3742s, 3128s, 1626s, 1566s, 1478s, 1416s, 1363s, 1203s, 1107s, 1008s, 741s, 493s, 445s.

$[Zn_{3.5}(\mu_3\text{-}OH)L_2(BTEC)(H_2O)]\cdot H_2O$ (**5**). To 10 mL of distilled water was added $Zn(OAc)_2\cdot 2H_2O$ (0.2 mmol), H_4BTEC (0.1 mmol) and L (0.1 mmol) while stirring. When the pH value of the mixture was adjusted to about 6.0 with NaOH solution (1.0 mol L^{-1}), then the mixture was placed in a 23 mL Teflon-lined stainless steel vessel, and heated at 150 °C for 72 h, and then the reaction system was cooled to room temperature at a rate of 5 °C/h. Crystals of **5** were obtained in yield (based on Zn): 56%. Anal. Calcd. for

$C_{42}H_{31}N_6O_{15}Zn_{3.5}$: C, 44.93; H, 2.76; N, 8.73%. Found: C, 44.98; H, 2.73; N, 8.70%. IR data (KBr, cm^{-1}): 3425s, 1613s, 1501s, 1455s, 1434s, 1400s, 1140s, 760s, 704s, 625s, 521s, 459s.

2.4. X-ray crystallographic studies

Single-crystal X-ray diffraction data for compounds **1–5** were recorded on a Bruker Apex CCD diffractometer with graphite-monochromated Mo$K\alpha$ radiation (λ=0.71073 Å) at 293 K. Absorption corrections were applied using multi-scan technique. All the structures were solved by direct method of SHELXS-97 [30] and refined by full-matrix least-squares techniques using the SHELXL-97 program [31] within WINGX [32]. Non-hydrogen atoms were refined with anisotropic temperature parameters. The disordered O atoms of the water molecules (O1W) in compound **3** and (O2W, O3W, O4W) in compound **4** were refined with isotropic temperature parameters. The disordered O atoms of the water molecules (O1W) in compound **3** and (O3W, O4W) in compound **4** were refined using O atoms split over two sites, with a total occupancy of 1, while (O2W) in compound **4** was refined using O atoms split over two sites, with a total occupancy of 0.5. The hydrogen atoms of the organic ligands were refined as rigid groups. Hydrogen atoms of water molecules were located from difference Fourier maps. The detailed crystallographic data and structure refinement parameters for **1–5** are summarized in Table S1 (Supporting Information), and selected bond lengths and angles are listed in Table S2 (Supporting Information). Crystallographic data for the structural analysis have been deposited with the Cambridge Crystallographic Data Center CCDC reference numbers 724698-724702.

3. Results and discussion

3.1. Preparation of compounds 1−5

In this system, the pH value of solution plays a crucial role in construction of compounds **1–5**. In our first attempts, we only obtained a small quantity of microcrystals unsuitable for single-crystal X-ray diffraction under the hydrothermal conditions. Then, we sensed that changing the pH value of the reaction mixture may be helpful for crystal growth. In view of this, we adjust the pH value of the reaction system. As expected, at pH 6–7 well-formed single crystals of **1–5** that are suitable for single-crystal X-ray diffraction were obtained. The reported pH value in the experimental section is the best choice, based on the yield. The hydrothermal reactions $Zn(OAc)_2\cdot 2H_2O$ and L generated compound **1**. The structure of **1** is relatively simple, which is a 1D double-bridged chain structure. According to previous reports, the chelating N-donor ligands may inhibit the expansion of polymetric framework, and compound **1** possesses a predictable low-dimension structure as most of the coordination polymers with similar ligands [33–35]. This result prompted us to extend our work by using other auxiliary ligands, especially those bridging ligands such as polycarboxylate aromatic acid. It is well-known that the structure geometry could be controlled and modulated by selecting some appropriate organic ligands [36]. We were interested in such reactions in the presence of auxiliary ligands and hoped to obtain the other novel architectures. Fortunately, compounds **2–5** were obtained under similar reaction conditions when different auxiliary ligands (1,3-benzenedicarboxylic acid, 1,4-benzenedicarboxylic acid, 1,3,5-benzenetricarboxylic acid, 1,2,4,5-benzenetetracarboxylic acid) were added.

3.2. Structural description of compounds 1−5

$[Zn(L)_2]\cdot$(1). Single-crystal X-ray structural analysis reveals that **1** crystallizes in the monoclinic space group ($P2_1/n$). The coordination environment of metal center is depicted in Fig. 1a. Each Zn^{II} center exhibits a distorted trigonal bi-pyramid geometry, being ligated by two carboxylic oxygen atoms (Zn1–O=1.9418(18)–2.0132(19) Å) from two distinct L ligands and three nitrogen atoms (Zn1–N=2.033(2)–2.458(2) Å) from another two different L ligands. The Zn–O/N bond lengths are all consistent with corresponding bond lengths found in the literature [37]. Compound **1** contains a 1D chain linked via double L bridges, as shown in Fig. 1b. L ligand adopts two kinds of coordination modes. Firstly, each L ligand coordinates to two Zn^{II} ions with two N and one O by chelate–monodentate coordination mode (Scheme 2a). Secondly, each L ligand coordinates to two Zn^{II} ions with one N and one O by monodentate–monodentate coordination mode (Scheme 2b). Consequently, two L ligands link two Zn^{II} ions to construct a metallic cycle as the based building block of the 1D chain with the Zn⋯Zn separation across the L ligand of 11.338 Å.

An interesting point is the presence of supramolecular interactions between such L ligands. The approximately parallel orientation of the L ligands allows neighboring related single-stranded chains to generate a supramolecular layer under the

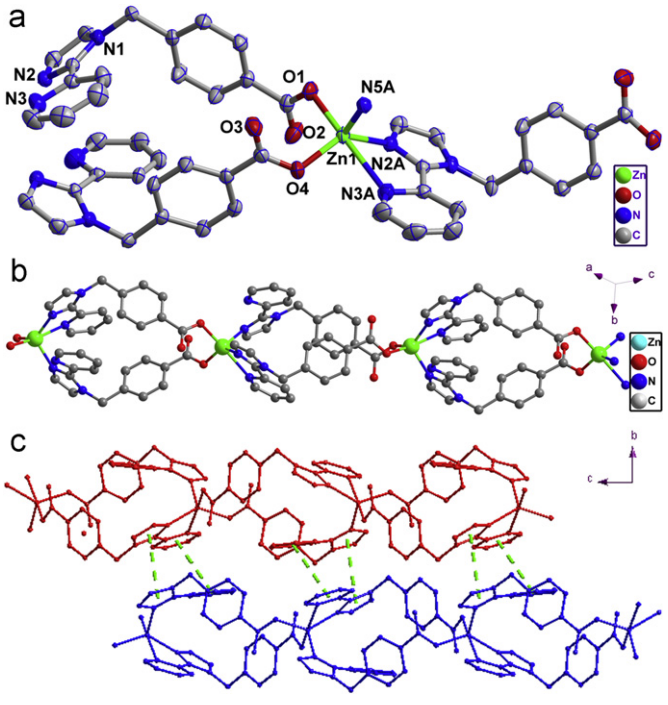

Fig. 1. (a) Coordination environment of Zn^{II} atoms in **1** with the ellipsoids drawn at the 50% probability level, symmetry code: A: $-0.5+x$, $0.5-y$, $0.5+z$; hydrogen atoms were omitted for clarity. (b) 1D double-bridged chain of compound **1**. (c) The 2D supramolecular of **1** formed through $\pi-\pi$ interactions.

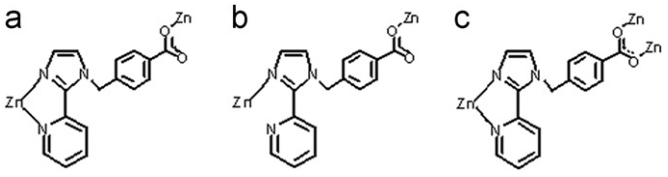

Scheme 2. The coordinated modes of the L ligand.

direction of aromatic $\pi\cdots\pi$ stacking interactions among the L pairs, with the plane to plane distance of 3.721 Å of two imidazole rings and the centroid–centroid distance of 3.940 Å of two pyridine rings (Fig. 1c). So an interesting 2D supramolecular layer is finally formed by linking these chains through $\pi\cdots\pi$ interactions.

[Zn_2(μ_3-OH)L(*m*-BDC)] (**2**). When *m*-H_2BDC ligand was introduced, a significantly different framework **2** was formed. Single-crystal X-ray diffraction study reveals that **2** contains tetranuclear zinc clusters, in which the μ_3-OH groups interlink three independent Zn^{II} ions, with non-bonding Zn···Zn separations of 3.152–3.676 Å. The asymmetric unit consists of two kinds of Zn^{II} ions, one L ligand, one *m*-BDC ligand and one coordinated μ_3-OH group (Fig. 2a). The Zn1 displays a distorted octahedral geometry, which is completed by two carboxylic oxygen atoms (Zn1–O=2.133(2)–2.144(2) Å) from one *m*-BDC ligand and one L ligand, two nitrogen atoms (Zn1–N=2.086(3)–2.200(3) Å) from one L ligand, and two μ_3-O atoms (Zn1–O=2.079(2)–2.142(2) Å), whereas Zn2 exists in a distorted tetrahedral sphere, being ligated by three carboxylic oxygen atoms (Zn2–O=1.931(2)–1.982(2) Å) from two different *m*-BDC ligands and one L ligand, and one μ_3-O atom (Zn2–O7=1.971(2) Å). Obviously, bond lengths in a tetrahedral geometry are shorter than those in octahedral geometries, which is consistent with those reported in the literature [38]. Different from compound **1**, each L ligand in **2** adopts chelate-bis(monodentate) coordination fashions to coordinate to three Zn^{II} ions with two N and two O donors (Scheme 2c). One carboxylate group of the *m*-BDC ligand adopts bidentate coordination fashion to bridge Zn1 and Zn2, and another carboxylate group adopts monodentate bridging mode to coordinate to Zn2 (Scheme 3a). Based on these connection modes, the L and *m*-BDC connect the adjacent tetranuclear zinc cluster to form a 3D framework (Fig. 2b). A better insight into the nature of the involved framework can be achieved by application of a topological approach, when we take the tetranuclear zinc cluster as a single six-connected node, due to two pairs of *m*-BDC ligands linking two adjacent tetranuclear zinc clusters (Supporting Information Fig. S1a), each organic ligand is regarded as a linear linker, therefore, the network can be simplified to a distorted 3D α-Po topology, as shown in Fig. 2c.

[Zn_2(μ_3-OH)L(*p*-BDC)] (**3**). When *p*-H_2BDC ligands were used instead of *m*-H_2BDC ligands to react with zinc ions, compound **3** possessing a 3D network was obtained. Single-crystal X-ray analysis reveals that the structure of **3** also contains tetranuclear zinc clusters, in which each μ_3-OH is attached to three independent Zn^{II} ions, with non-bonding Zn···Zn distances of 3.155–3.696 Å. As shown in Fig. 3a, there are two crystallographically unique Zn^{II} centers in the asymmetric unit. Zn1 is six-coordinated and shows a slightly distorted octahedral coordination geometry, which is finished by two carboxylic oxygen atoms (Zn1–O=2.121(2)–2.123(2) Å) from one L ligand and one *p*-BDC ligand, two nitrogen atoms (Zn1–N=2.105(2)–2.192(2) Å) from one L ligand, and two μ_3-O atoms (Zn1–O=2.094(2)–2.161(2) Å), whereas Zn2 exhibits a distorted tetrahedral geometry, being bound by three carboxylic oxygen atoms (Zn2–O=1.935(2)–1.982(2) Å) from two different *p*-BDC and one L, and one μ_3-O atom (Zn2–O7=1.962(19) Å). The L ligands adopt the same coordination mode as that of **2** (Scheme 2c). Moreover, coordination mode of *p*-BDC ligand is similar to that coordination fashion of *m*-BDC in compound **2**, as shown in Scheme 3b. Such tetranuclear zinc clusters are connected through L and *p*-BDC ligands into a 3D framework as shown in Fig. 3b. Topological analysis of this compound reveals

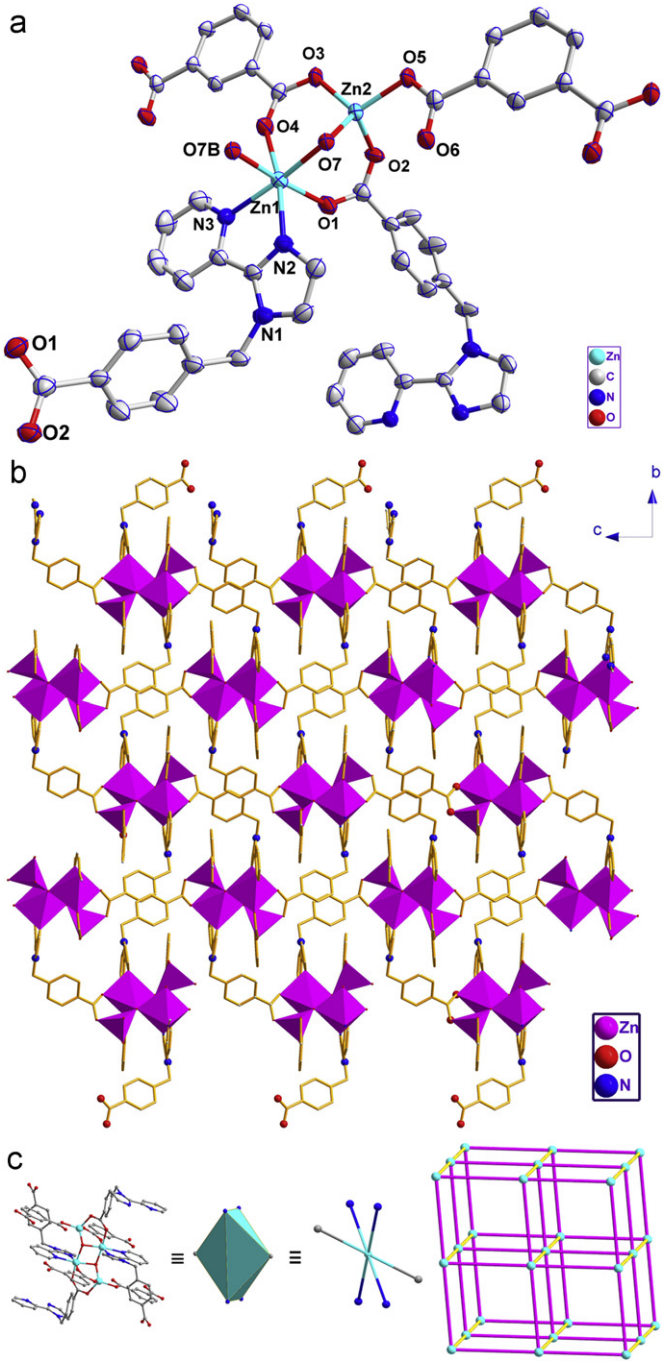

Fig. 2. (a) Coordination environment of Zn^{II} atoms in **2** with the ellipsoids drawn at the 50% probability level, symmetry code: A: 0.5+*x*, 0.5−*y*; 0.5+*z*; B: −*x*, −*y*, −*z*; hydrogen atoms were omitted for clarity. (b) Perspective views of the stacking arrays of **2**. (c) Topological representation of **2** showing the α-Po topology.

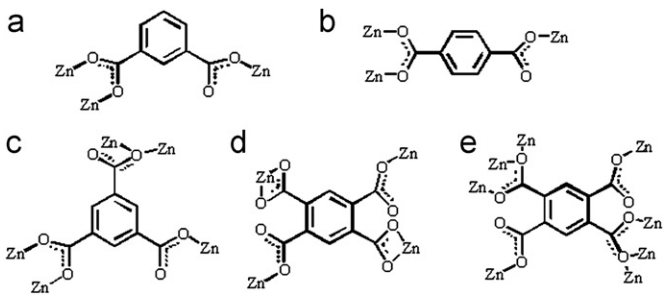

Scheme 3. The coordinated mode of the poly carboxylate ligands.

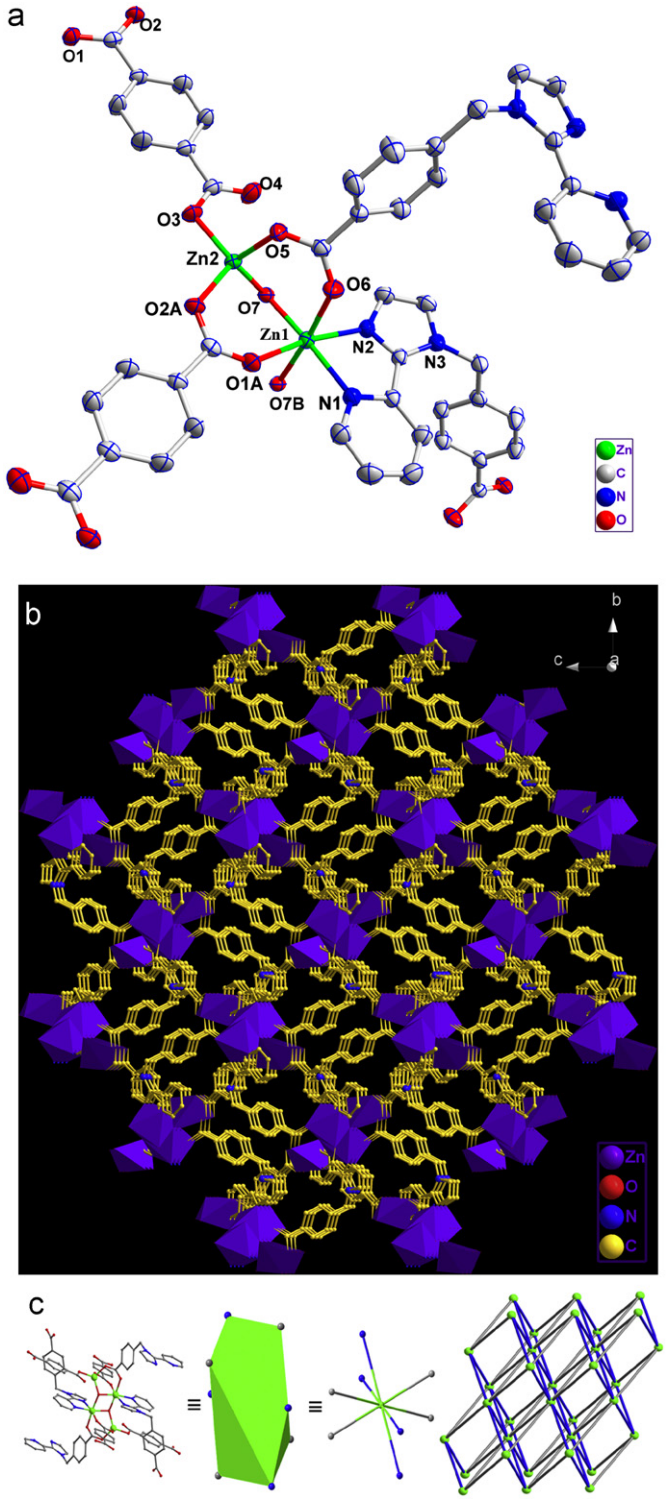

Fig. 3. (a) Coordination environment of Zn^{II} atoms in **3** with the ellipsoids drawn at the 50% probability level, symmetry code: A: 0.5+*x*, −0.5−*y*, −0.5+*z*, B: −*x*, −*y*, 1−*z*; hydrogen atoms were omitted for clarity. (b) Perspective views of the stacking arrays of **3**. (c) Topological representation of **3** showing the bcu network.

that it is a uninodal bcu net with $(4^{24}\cdot 6^4)$ topology, if the tetranuclear Zn_4 unit bridging four L and four *p*-BDC ligands is considered as 8-connected node (Supporting Information Fig. S1b), while L ligands and *p*-BDC ligands are regarded as linear linkers.

The crystal structures of compounds **2** and **3** are intriguing and prompt us to explore the generality of producing grid network with the ligand of bent configuration of ligating atoms, such as H_3BTC and H_4BTEC.

$[Zn_2L(BTC)(H_2O)]\cdot 2.5H_2O$ (**4**). A single-crystal X-ray diffraction study reveals that compound **4** crystallizes in the orthor-

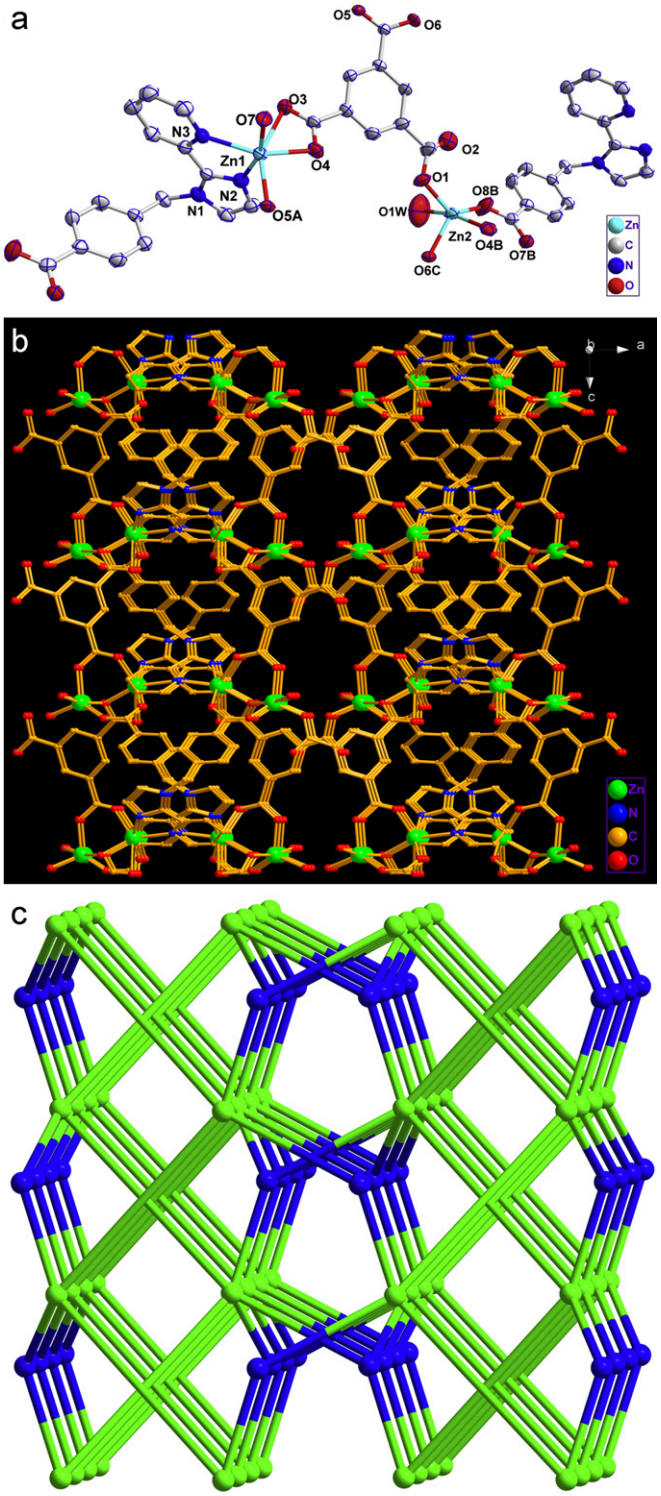

Fig. 4. (a) Coordination environment of Zn^{II} atoms in **4** with the ellipsoids drawn at the 50% probability level, symmetry code: A: *x*, −*y*+2, *z*−1/2; B: −*x*+1, −*y*+2, *z*; C: −*x*+1, *y*, *z*−1/2; hydrogen atoms were omitted for clarity. (b) Perspective views of the stacking arrays of **4**. (c) Schematic view of the 3D (3,5)-connected network of $(4\cdot 6^2)(4\cdot 6^4\cdot 8^2\cdot 10\cdot 12^2)$ topology, green ones are the metal dinuclear zinc cluster and blue ones are the BTC ligands. (For interpretation of the references to color in this figure legend, the reader is referred to the web version of this article.)

hombic space group *Iba*2. As shown in Fig. 4a, there are two crystallographically unique Zn^{II} centers in the asymmetric unit. Each Zn1 is six-coordinated by four carboxylic oxygen atoms (Zn1–O=2.040(4)–2.442(5) Å) from two BTC ligands and one L, and two nitrogen atoms (Zn1–N=2.080(2)–2.176(5) Å) from one L ligand, shows a distorted octahedral geometry, whereas Zn2 exhibits a distorted trigonal bi-pyramidal sphere, being completed by four carboxylic oxygen atoms (Zn2–O=1.894(5)–2.179(4) Å) from three different BTC ligands and one L ligand, and one coordinated water molecule (Zn2–O1w=2.277(8) Å). The L ligand in **4** also adopts chelate-bis(monodentate) coordination fashions (Scheme 2c). The carboxylate groups of completely deprotonated BTC ligand display three kinds of coordination fashions, namely, bidentate, monodentate and monodentate-bridging to two zinc centers (Scheme 3c). The adjacent zinc atoms are interlinked by three carboxylate groups from two BTC ligands and one L ligand to construct a dinuclear zinc cluster, in which the Zn···Zn distance is 3.394 Å (Supporting Information Fig. S2). Furthermore, the dinuclear zinc clusters are in turn connected by BTC and L to give rise to the complicated 3D framework, as shown in Fig. 4b. Better insight into such elegant frameworks can be accessed by the topology method: the dinuclear zinc cluster linking two L and three BTC ligands forms a 5-connected node, while each BTC ligand connecting three dinuclear zinc clusters acts as a 3-connected node. So the whole framework can be described as a novel 3D (3,5)-connected network with the Schläli symbol of $(4\cdot6^2)(4\cdot6^4\cdot8^2\cdot10\cdot12^2)$, as shown in Fig. 4c. To our knowledge, only a few (3,5)-connected coordination polymers have been reported until now [39–43].

$[Zn_{3.5}(\mu_3\text{-}OH)L_2(BTEC)(H_2O)]\cdot H_2O$ (5). Compared with compound **4**, the H_3BTC ligands were replaced by H_4BTEC ligands, and the resulting structure was an intricate 3D framework. Compound **5** crystallizes in the triclinic space group $P-1$. There are four crystallographically independent Zn^{II} centers with three coordination environments in **5**, as shown in Fig. 5a. The Zn1 is coordinated by four carboxylic oxygen atoms (Zn1–O=1.937(4)–2.457(6) Å) from one L and two BTEC ligands, and one μ_3-O atom (Zn1–O13=2.018(4) Å) to construct a distorted trigonal bi-pyramidal environment; while the Zn2 is finished by three carboxylic oxygen atoms (Zn2–O=1.988(4)–2.484(4) Å) from one BTEC and two distinct L ligands, two nitrogen atoms (Zn2–N=2.057(5)–2.123(5) Å) from one L ligand, and one μ_3-O atom (Zn2–O13=2.059(4) Å) giving a distorted octahedral geometry; the Zn3 also exists in an octahedral geometry, being ligated by four carboxylic oxygen atoms (Zn3–O=2.243(4)–2.253(4) Å) from two distinct BTEC ligands and two L ligands, two μ_3-O atoms (Zn3–O=1.946(4) Å); similar to Zn1, the Zn4 atom also adopts a distorted trigonal bi-pyramidal geometry, being finished by two carboxylic oxygen atoms (Zn4–O=1.976(5)–2.078(4) Å) from two BTEC ligands, two nitrogen atoms (Zn4–N=1.944(5)–2.363(6) Å) from one L ligand, and one coordinated water molecule (Zn4–O2W=2.008(5) Å). The L ligand adopts coordination fashion is same to that of **2** (Scheme 2c). The BTEC ligand adopts two kinds of coordination fashions. Firstly, the BTEC ligand acts as a tetradentate ligand, two carboxyl groups adopt monodentate towards Zn^{II} centers with O atoms connecting Zn4 and the other two carboxyl groups adopt bis-chelating fashions towards Zn^{II} centers with O atoms connecting Zn1 (Scheme 3d). Secondly, the BTEC ligand acts as an octadentate ligand, two carboxyl groups adopt monodentate towards Zn^{II} centers with O atoms connecting Zn4 and the other two carboxyl groups adopt tridentate fashions towards Zn^{II} centers with O atoms connecting Zn1, Zn2 and Zn3 (Scheme 3e).

It is interesting to note two μ_3-OH groups and six carboxylate groups interlink three crystallographically unique Zn^{II} ions to construct a pentanuclear zinc cluster, with non-bonding Zn···Zn distances of 3.185–3.387 Å (Supporting Information Fig. S3a).

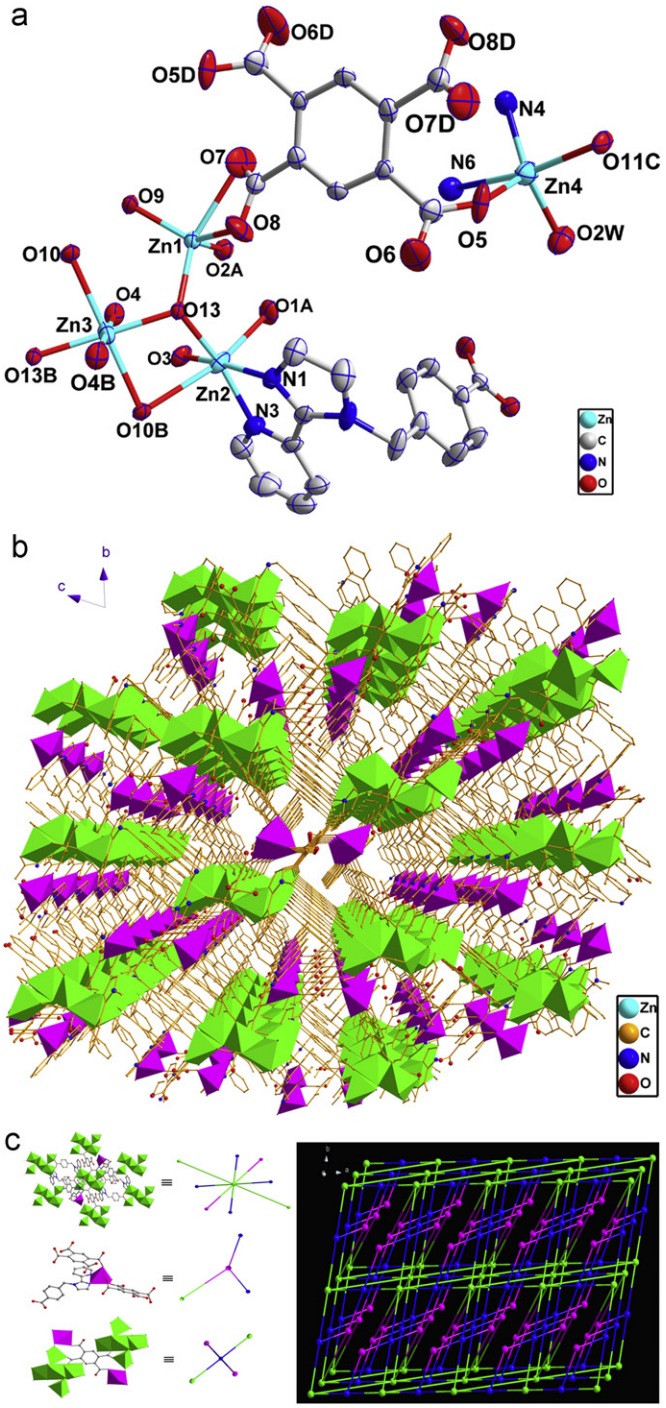

Fig. 5. (a) Coordination environment of Zn^{II} atoms in **5** with the ellipsoids drawn at the 50% probability level, symmetry code: A: $-x+2$, $-y$, $-z$; B: $-x+1$, $-y$, $-z+1$; C: $x+1$, $y+1$, $z-1$; D: $-x+1$, $-y+1$, $-z$; hydrogen atoms were omitted for clarity. (b) Perspective views of the stacking arrays of **5** along *a* axis. (c) Schematic view of the 3D (3,4,8)-connected network of $(4\cdot6^2)(4^2\cdot6^3\cdot8)(4^2\cdot6^4)(4^2\cdot6^{18}\cdot7\cdot8^6\cdot10)$ topology, with green stick representing pentanuclear metal clusters, pink ones represent Zn4 centers and blue ones represent the BTEC ligands. (For interpretation of the references to color in this figure legend, the reader is referred to the web version of this article.)

Based on above connection modes, the L and BTEC ligands connect the adjacent pentanuclear metal clusters and Zn4 centers to form a 3D framework, as shown in Fig. 5b. From the topological point of view, each pentanuclear metal cluster is surrounded by 10 organic ligands-four bridging BTEC and six L ligands (Supporting Information Fig. S3b). Due to two pairs of L ligands linking two adjacent

pentanuclear metal clusters, therefore, pentanuclear metal cluster is defined as an eight-connected node, while each Zn4 connecting two BTEC ligands and one L ligand acts as a 3-connected node, each BTEC ligand bridging two pentanuclear metal clusters and two Zn4 ions acts as a 4-connected node. So the whole framework can be described as a (3,4,8)-connected network with the Schläli symbol of $(4\cdot6^2)(4^2\cdot6^3\cdot8)(4^2\cdot6^4)(4^2\cdot6^{18}\cdot7\cdot8^6\cdot10)$, as shown in Fig. 5c. Although a large number of high-connected structures have been documented [44–47], to our knowledge, (3,4,8)-connected framework has been not reported until now.

3.3. Auxiliary aromatic-acid effect on the structure of the compounds

The effects of auxiliary aromatic-acid ligands on the molecular structures of the resulting compounds **2–5** have been clearly demonstrated. Through varying auxiliary aromatic-acid ligands under similar synthesis conditions, four related zinc compounds were successfully isolated and they exhibit significant differences in their molecular architecture. It is well-known that the role of organic ligands can be explained in terms of their differences in shape, size, and flexibility. In this study, diverse polycarboxylate aromatic acids were used to investigate their influence on the structure of the zinc compounds. It is obvious from the above descriptions that the auxiliary ligands (1,3-benzenedicarboxylic acid, 1,4-benzenedicarboxylic acid, 1,3,5-benzenetricarboxylic acid, 1,2,4,5-benzenetetracarboxylic acid) have significant effects on the final structures of the resulting compounds. When *m*-H_2BDC ligands were introduced, a 3D α-Po framework **2** was formed. When *p*-H_2BDC ligands were used instead of *m*-H_2BDC ligands, structurally different 3D bcu framework **3** was formed under similar reaction conditions. The structural differences between **2** and **3** showed the importance of the dicarboxylic acid position on the compound construction, even though the coordination modes of L and auxiliary aromatic-acid ligands are the same (L ligand adopts chelate-bis(monodentate) coordination fashions, and *m*-BDC/*p*-BDC ligand adopts monodentate-bidentate coordination fashion). Compound **4** or **5** was also constructed when H_3BTC or H_4BTEC ligands were used instead of *m*-H_2BDC ligands under similar reaction conditions, respectively. The structural differences between compounds **4** and **5** showed the importance of the carboxylic unit numbers on the compound construction. In compounds **4** and **5**, L ligand also adopts chelate-bis(monodentate) coordination fashions, while auxiliary aromatic-acid ligands adopt obviously different coordination fashion. In **4**, the H_3BTC ligand adopts monodentate, bidentate and monodentate-bridging to two metal centers coordination modes. In **5**, the H_4BTEC ligand shows an intricate coordination fashions: (i) the BTEC ligand acts as a tetradentate ligand, adopt bis(monodentate)-bis(chelating) fashions; (ii) the BTEC ligand acts as an octadentate ligand, adopt bis(monodentate)-bis(tridentate). These results indicate that the formation of **2–5** under similar reaction conditions depends primarily on the chemical nature of the auxiliary aromatic-acid ligands. These may be attributed to the different shapes of the polycarboxylate ligands. The *m*-H_2BDC, *p*-H_2BDC, H_3BTC and H_4BTEC ligands are with different angles between the two carboxylate groups and different carboxylate units, which favor the formation of coordination polymers. Using the proper choice of the diversely shaped ligands and central metal ions, various dimensional networks can be developed.

3.4. Thermal stability properties of the compounds

In order to characterize the compounds more fully in terms of thermal stability, their thermal behaviors were studied by TGA. The experiments were performed on samples consisting of numerous single crystals of compounds **1–5** under N_2 atmosphere with a heating rate of 10 °C/min (Supporting Information Fig. S4). The TGA curve of compounds **1–2** both indicate that one weight loss stage exists in the region of 342–458 °C for **1** and 312–489 °C for **2**, the anhydrous compound decomposes with a step-wise loss of the organic composition, respectively. The TGA curve of **3** shows that it undergoes dehydration in the temperature range of 15–102 °C. This corresponds to the loss of water molecules (obsd. 2.96%, calcd. 3.12%). From 334 to 485 °C, the anhydrous compound decomposes with a step-wise loss of the organic composition. TGA curve of **4** shows that a weight loss of 9.48% (calcd. 9.27%) corresponding to the loss of two solvent water molecules and one coordinated water molecule was observed between 18 and 110 °C, and the anhydrous compound decomposes with a step-wise loss of the organic composition above 368 °C. TGA curve of **5** shows that a weight loss of 3.38% (calcd. 3.20%) corresponding to the loss of one solvent water molecule and one coordinated water molecule was observed between 25 and 118 °C, and the anhydrous compound decomposes with a step-wise loss of the organic composition above 343 °C.

3.5. Solid-state fluorescence spectroscopy

Luminescent compounds are of great current interest because of their various applications in chemical sensors, photochemistry and electroluminescent display [48,49]. The photoluminescent spectra of compounds **1–5** and free ligand L measured at room temperature are depicted in Fig. 6, and the wavelengths of the emission maximums and excitation are listed in Table S3 (Supporting Information). It can be observed that intense emissions occur at 388 nm (λ_{ex}=350 nm) for **1**, 398 nm (λ_{ex}=350 nm) for **2**, 390 nm (λ_{ex}=340 nm) for **3**, 386 nm (λ_{ex}=340 nm) for **4** and 384 nm (λ_{ex}=350 nm) for **5**. To understand the nature of the two emission bands, we analyzed the photoluminescence properties of the L ligand and found that the strongest emission peak for L is at about 404 nm (λ_{ex}=344 nm). Moreover, solid-state aromatic carboxylate ligands can also exhibit fluorescent properties at room temperature reported by the literature, the main emission peak for 1,3-H_2BDC is located at 370 nm (λ_{ex}=327 nm) [50], 1,4-H_2BDC is located at 380 nm (λ_{ex}=350 nm) [51], H_3BTC is located at 380 nm (λ_{ex}=334 nm) [52], H_4BTEC is located at 370 nm

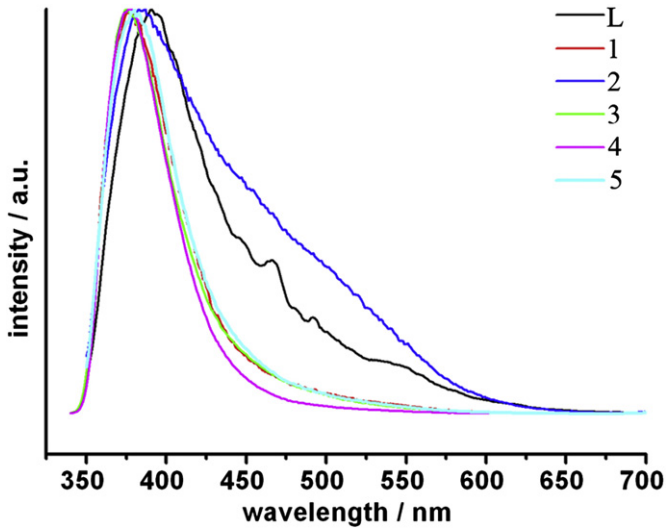

Fig. 6. Solid-state photoluminescent spectra of L ligand, and compounds **1–5** at room temperature.

(λ_{ex}=327 nm) [53]. The emission bands of aromatic carboxylate ligands may be attributable to the $\pi^* \rightarrow n$ transitions. Interestingly, the emission spectra for the zinc coordination polymers show the main peaks at ~390 nm. These peaks correspond to the intra-ligand fluorescent emission [54]. These results imply that the coordination of the L and aromatic aromatic carboxylate ligands with the zinc ions, although yielding different topological structures, has no influence on the emission mechanism of the MOFs [55–57].

3.6. IR spectra

In their IR spectra, the absorption bands resulting from the skeletal vibrations of the aromatic ring were observed in the 1400–1600 cm^{-1} region. The absence of the characteristics bands at 1715–1680 cm^{-1} indicates the complete deprotonation of the five carboxylic acids by NaOH upon reaction with Zn ions, which is also consistent with the X-ray diffraction results. Moreover, the strong vibrations appearing around 1614 and 1416 cm^{-1} corresponding to the asymmetric and symmetric stretching vibrations of the carboxylate group, respectively. The separations (Δ) between ν_{asym} (CO_2) and ν_{sym} (CO_2) indicate that the presence of bridging monodentate coordination mode of the carboxylate group in compounds **1–5** [58,59], which is also confirmed by single-crystal structure analysis. In addition, the FT-IR spectra of **2–4** have strong peaks at 3742–3113 cm^{-1}, respectively, which can be attributed that O–H stretch of lattice and coordinated water molecules.

3.7. XRPD results

In order to substantiate the phase purity of the as-synthesized compounds **1–5**, their X-ray powder diffraction (XRPD) measurement also was performed. The XRPD experimental and computer-simulated patterns of the corresponding compounds are shown in Supporting Information, Fig. S5. The experimental XRPD patterns are in good agreement with the corresponding simulated ones except for the relative intensity variation because of preferred orientations of the crystals.

4. Conclusions

In summary, we have successfully isolated five interesting polymeric networks constructed from the zinc ions and L ligands under hydrothermal conditions. We have indicated our aim of coordination polymer synthesis. Compounds **2–5** with 3D network were formed in the presence of auxiliary aromatic-acid ligands, while compound **1** with 1D chain was obtained in the absence of auxiliary aromatic-acid ligands. The structural discrimination among **2–5** indicates the influence of carboxylate numbers and carboxylate position of aromatic-acid ligands on structure formation of their compounds. The difference in coordination modes of the aromatic polycarboxylic acids and the versatile conformation of L exert an important influence on the resulting frameworks. The results also present a feasible strategy for controlling the synthesis of framework architectures by organic ligand design. Moreover, compounds **1–5** display blue emissions at room temperature; therefore, they may appear to be candidates for novel hybrid inorganic-organic photoactive materials. Further studies are now under way in our laboratory.

Acknowledgments

We are thankful for financial support from the Program for Changjiang Scholars and Innovative Research Team in University, the National Natural Science Foundation of China (nos. 20573016, 20901014 and 20703008), the Science Foundation for Young of Jilin Scientific Development Project (nos. 20090125 and 20090129), the Science Foundation for Young Teachers of NENU (no. 20090407), the Training Fund of NENU's Scientific Innovation Project (NENU-STC08019), Ph.D. Station Foundation of Ministry of Education for New Teachers (no. 20090043120004), the Postdoctoral Foundation of Northeast Normal University, and the Postdoctoral Foundation of China (no. 20090461029).

Appendix A. Supplementary material

Supplementary data associated with this article can be found in the online version at 10.1016/j.jssc.2010.01.027.

References

[1] O.M. Yaghi, M. O'Keeffe, N.W. Ockwig, H.K. Chae, M. Eddaoudi, J. Kim, Nature 423 (2003) 705.
[2] N.W. Ockwig, O. Delgado-Friederichs, M. O'Keeffee, O.M. Yaghi, Acc. Chem. Res. 38 (2005) 176.
[3] Z. Wang, V.C. Kravtsov, M.J. Zaworotko, Angew. Chem. Int. Ed. 44 (2005) 2877.
[4] S.R. Batten, R. Robson, Angew. Chem. Int. Ed. 37 (1998) 1460.
[5] L. Carlucci, G. Ciani, D.M. Proserpio, Coord. Chem. Rev. 246 (2003) 247.
[6] R.J. Hill, D.L. Long, N.R. Champness, P. Hubberstey, M. Schröder, Acc. Chem. Res. 38 (2005) 337.
[7] B. Moulton, M.J. Zaworotko, Chem. Rev. 101 (2001) 1629.
[8] J. Wu, Y.L. Song, E.P. Zhang, H.W. Hou, Y.T. Fan, Y. Zhu, Chem. Eur. J. 12 (2006) 5823.
[9] Q.R. Fang, G.S. Zhu, M. Xue, J.Y. Sun, F.X. Sun, S.L. Qiu, Inorg. Chem. 45 (2006) 3582.
[10] M. Fujita, Y.J. Kwon, S. Washizu, K. Ogura, J. Am. Chem. Soc. 116 (1994) 1151.
[11] H.W. Park, S.M. Sung, K.S. Min, H. Bang, M.P. Suh, Eur. J. Inorg. Chem. (2001) 2857.
[12] S.J. Deng, N. Zhang, W.M. Xiao, C. Chen, Inorg. Chem. Commun. 12 (2009) 157.
[13] J.F. Song, Y. Chen, Z.G. Li, R.S. Zhou, X.Y. Xu, J.Q. Xu, J. Mol. Struct. 842 (2007) 125.
[14] O.S. Jung, Y.J. Kim, Y.A. Lee, J.K. Park, H.K. Chae, J. Am. Chem. Soc. 122 (2000) 9921.
[15] C. He, B.G. Zhang, C.Y. Duan, J.H. Li, Q.J. Meng, Eur. J. Inorg. Chem. (2000) 2549.
[16] R. Horikoshi, T. Mochida, H. Moriyama, Inorg. Chem. 40 (2001) 2430.
[17] X.Q. Liang, X.H. Zhou, C. Chen, H.P. Xiao, Y.Z. Li, J.L. Zuo, X.Z. You, Cryst. Growth Des. 9 (2009) 1041.
[18] M. Eddaoudi, D.B. Moler, H. Li, B. Chen, T.M. Reineke, M. O'Keeffe, O.M. Yaghi, Acc. Chem. Res. 34 (2001) 319.
[19] R.H. Wang, M.C. Hong, D.Q. Yuan, Y.Q. Sun, L.J. Xu, J.H. Luo, R. Cao, A.S.C. Chan, Eur. J. Inorg. Chem. (2004) 37.
[20] S.S.Y. Chui, S.M.F. Lo, J.P.H. Charmant, A.G. Orpen, I.D. Williams, Science 283 (1999) 1148.
[21] Z. Shi, G. Li, L. Wang, L. Gao, X. Chen, J. Hua, S. Feng, Cryst. Growth Des. 4 (2004) 25.
[22] M. Eddaoudi, D.B. Moler, H. Li, B. Chen, T.M. Reineke, M. O' Keeffe, O.M. Yaghi, Acc. Chem. Res. 34 (2001) 319.
[23] H.W. Roesky, M. Andruh, Coord. Chem. Rev. 236 (2003) 91.
[24] J.J. Wang, L. Gou, H.M. Hu, Z.X. Han, D.S. Li, G.L. Xue, M.L. Yang, Q.Z. Shi, Cryst. Growth Des. 7 (2007) 1514.
[25] Y. Zheng, M. Du, J.R. Li, R.H. Zhang, X.H. Bu, J. Chem. Soc. Dalton Trans. (2003) 1509.
[26] J. Yang, J.F. Ma, Y.Y. Liu, J.C. Ma, H.Q. Jia, N.H. Hu, Eur. J. Inorg. Chem. (2006) 1208.
[27] J. Yang, J.F. Ma, Y.Y. Liu, J.C. Ma, S.R. Batten, Cryst. Growth Des. 8 (2008) 4383.
[28] L.S. Long, K.Y. Ding, X.M. Chen, L.N. Ji, Inorg. Chem. Commun. 3 (2000) 65.
[29] I. Bertini, P. Turano, A. Vila, Chem. Rev. 93 (1993) 2833.
[30] G.M. Sheldrick, SHELXS-97, Programs for X-ray Crystal Structure Solution, University of Göttingen, Göttingen, Germany, 1997.
[31] G.M. Sheldrick, SHELXL-97, Programs for X-ray Crystal Structure Refinement, University of Göttingen, Göttingen, Germany, 1997.
[32] L.J. Farrugia, WINGX, A Windows Program for Crystal Structure Analysis, University of Glasgow, Glasgow, UK, 1988.
[33] Q. Shi, R. Cao, D.F. Sun, M.C. Hong, Y.C. Liang, Polyhedron 20 (2001) 3287.
[34] L.J. Zhang, J.Q. Xu, Z. Shi, X.L. Zhao, T.G. Wang, J. Solid State Chem. 32 (2003) 32.

[35] X. He, C.Z. Lu, D.Q. Yuan, L.J. Chen, Q.Z. Zhang, C.D. Wu, Eur. J. Inorg. Chem. (2005) 4598.
[36] R.H. Wang, L. Han, F.L. Jiang, Y.F. Zhou, D.Q. Yuan, M.C. Hong, Cryst. Growth Des. 5 (2005) 129.
[37] R.Q. Fang, X.M. Zhang, Inorg. Chem. 45 (2006) 4801.
[38] J. Tao, X. Yin, Z.B. Wei, R.B. Huang, L.S. Zheng, Eur. J. Inorg. Chem. (2004) 125.
[39] H.Y. He, F.N. Dai, D.F. Sun, Dalton Trans. (2009) 763.
[40] R. Heck, J. Bacsa, J.E. Warren, M.J. Rosseinsky, D. Bradshaw, CrystEngComm 10 (2008) 1687.
[41] K.A. Brown, D.P. Martin, R.L. LaDuca, CrystEngComm 10 (2008) 1305.
[42] X.Y. Cao, J. Zhang, Z.J. Li, J.K. Cheng, Y.G. Yao, CrystEngComm 9 (2007) 806.
[43] B. Zheng, H. Dong, J.F. Bai, Y.Z. Li, S.H. Li, M. Scheer, J. Am. Chem. Soc. 130 (2008) 7778.
[44] J.J. Morris, B.C. Noll, K.W. Henderson, Chem. Commun. (2007) 5191.
[45] X.L. Wang, C. Qin, Y.Q. Lan, K.Z. Shao, Z.M. Su, E.B. Wang, Chem. Commun. (2009) 410.
[46] J.E. McGarrah, Y.J. Kim, M. Hissler, R. Eisenberg, Inorg. Chem. 40 (2001) 4510.
[47] M. Xue, G.S. Zhu, H. Ding, L. Wu, X.J. Zhao, Z. Jin, S.L. Qiu, Cryst. Growth Des. 9 (2009) 1481.
[48] Y.R. Liu, L. Li, T. Yang, X.W. Yu, C.Y. Su, CrystEngComm 11 (2009) 2712.
[49] G.D. Santis, L. Fabbrizzi, M. Licchelli, A. Poggi, A. Taglietti, Angew. Chem. Int. Ed. Engl. 35 (1996) 202.
[50] E.C. Yang, J. Li, B. Ding, Q.Q. Liang, X.G. Wang, X.J. Zhao, CrystEngComm 10 (2008) 158.
[51] W. Chen, J.Y. Wang, C. Chen, Q. Yue, H.M. Yuan, J.S. Chen, S. Ni. Wang, Inorg. Chem. 42 (2003) 944.
[52] J. Yang, Q. Yue, G.D. Li, J.J. Cao, G.H. Li, J.S. Chen, Inorg. Chem. 45 (2006) 2857.
[53] S.V. Ganesan, S.A. Natarajan, J. Chem. Sci. 116 (2004) 65.
[54] D.R. Xiao, E.B. Wang, H.Y. An, Y.G. Li, Z.M. Su, C.Y. Sun, Chem. Eur. J. 12 (2006) 6528.
[55] M.P. Clares, J. Aguilar, R. Aucejo, C. Lodeiro, M.T. Albelda, F. Pina, J.C. Lima, A.J. Parola, J. Pina, S. de Melo, C. Soriano, E. García-España, Inorg. Chem. 43 (2004) 6114.
[56] F. Bolletta, I. Costa, L. Fabbrizzi, M. Licchelli, M. Montalti, P. Pallavicini, L. Prodi, N. Zaccheroni, J. Chem. Soc. Dalton Trans. (1999) 1381.
[57] S.A. Zabin, C.R. Jejurkar, J. Polym. Mater. 14 (1997) 239.
[58] K. Nakamoto, Infrared Spectra and Raman Spectra of Inorganic and Coordination Compound, Wiley, New York, 1986.
[59] X.L. Wang, C. Qin, E.B. Wang, L. Xu, J. Mol. Struct. 737 (2005) 49.